Nanocoolers

J. Stat. Mech. (2011) P10026

(http://iopscience.iop.org/1742-5468/2011/10/P10026)

Journal of Statistical Mechanics: Theory and Experiment
An IOP and SISSA journal

Nanocoolers

Martin Horvat[1], Tomaž Prosen[1] and Giulio Casati[2,3]

[1] Department of Physics, Faculty of Mathematics and Physics, University of Ljubljana, Jadranska 19, SI-1000 Ljubljana, Slovenia
[2] CNISM, CNR-INFM & Center for Nonlinear and Complex Systems, Universita' degli Studi dell'Insubria, Via Valleggio 11, 22100 Como, Italy
[3] Istituto Nazionale di Fisica Nucleare, Sezione di Milano, Via Celoria 16, 20133 Milano, Italy
E-mail: martin.horvat@fmf.uni-lj.si, tomaz.prosen@fmf.uni-lj.si and giulio.casati@uninsubria.it

Received 25 July 2011
Accepted 27 September 2011
Published 24 October 2011

Online at stacks.iop.org/JSTAT/2011/P10026
doi:10.1088/1742-5468/2011/10/P10026

Abstract. We present a simple kinematic model of a non-equilibrium steady state device, which can operate either as a heat engine or as a refrigerator. The model is composed of two or more scattering channels where the motion is fully described by deterministic classical dynamics, which connect a pair of stochastic (infinite) heat and particle baths at unequal temperatures. We discuss precise kinematic conditions under which our model may approach Carnot's optimal efficiency in different situations.

Keywords: transport processes/heat transfer (theory), dynamical processes (theory), stochastic processes (theory), transport properties (theory)

J. Stat. Mech. (2011) P10026

1742-5468/11/P10026+22$33.00

Contents

1. Introduction

It has been recognized in recent years that an efficient energy conversion and transformation between heat and work on all scales, in particular at the nanoscale, poses one of the main challenges for future social needs. One of the most promising technologies is a thermoelectric circuit which can simply convert a heat flux from a hot to cold place into electrical power, or conversely, using the electrical power to pump heat from a cold to a hot place [1]. However, although such devices have been known for a long time, and even their technological applications have been diverse for several decades, their thermodynamic efficiency remains quite low compared to compressor-based refrigerators or fuel-burning internal combustion engines. One of the main reasons for such low efficiency is a rather poor theoretical understanding of the relatively low figure of merit, the so-called ZT, in all known materials at room temperature.

Recently, a dynamical systems approach has been proposed [5, 10] in an attempt to better understand the mechanism which could lead to an increase of ZT and thus of thermoelectric efficiency. Along these lines we propose here a mathematically simple, general model of a steady state thermoelectric device that can be analyzed theoretically within the framework of classical statistical mechanics. The model is composed of two or more classical two-port scattering channels where the motion (of non-interacting charged particles) is fully deterministic and energy conserving, and which connect two stochastic, infinite heat and particle baths at different temperatures. The motion in the longitudinal direction connecting the two baths is quasi-free, except for point scatterers in the middle of the channels, which have certain simple properties. Namely, the transmission depends

J. Stat. Mech. (2011) P10026

only on the (kinetic) energy of the particle. It is argued that the dependence on energy of the transmission (scattering) function is crucial in order to obtain non-vanishing efficiency. The particles are subjected only to a bias voltage that is used to input or output the work from the system.

The model we discuss here, although quite abstract, is the most general case of a self-contained (compact) classical heat engine model, composed of two thermo-chemical baths with non-interacting particles. Its simplicity allows theoretical analysis and therefore a better understanding of how a thermoelectric engine operates and the mechanism underlying the behavior of ZT. Indeed, in our paper we develop an easy-to-follow formalism in order to discuss particle and heat currents inside the model as well as its power and thermoelectric efficiency. The model's simplicity indicates that engines based on its principles could be built practically and, thus, the model may be important for the future design of heat engines.

More precisely, we derive analytical expressions for the engine's efficiency, power and the parameters that optimize efficiency (section 2). In the linear temperature difference regime (section 3), in particular, there are cases such as window-type scattering functions (section 5) that can be worked out exactly. It is particularly interesting that in the linear temperature difference regime, the refrigeration and power generation modes of operation can be treated symmetrically. Using our formalism, it is possible to discuss the precise conditions under which the model attains Carnot's efficiency. We show, in section 4, that the generalized figure of merit is essentially given as a ratio of the variance of the Seebeck coefficients for various channels divided by the average variance of the transmitted particle's energy. It is found that *narrow energy filtering* is a good mechanism for increasing the thermoelectric efficiency of the engines, based on our classical model. A similar effect was previously observed in quantum models, see e.g. [2]. In section 6, we work out semi-analytically and numerically a slightly different model of a thermoelectric engine where the scattering is provided by a homogeneous transverse magnetic field. In this setup, power and efficiency turn out to be tunable via the external magnetic field; however the maximal efficiency remains rather low.

Some more technical aspects of our formalism that are not essential for the main results are presented in two appendices. In appendix A, we present a consistent construction of classical scattering matrices and their concatenation for structured scattering channels. While most of the work in this paper refers to the steady state operation of heat engine models, we dedicate appendix B to the discussion of relaxation times to the steady state. In particular we show that non-vanishing bias voltages in all channels render strictly finite relaxation times.

As discussed in the following sections, our formalism allows an efficient numerical and analytical treatment of concrete non-trivial cases of classical–mechanical models of heat engines and helps us to identify the main transport properties controlling power generation and efficiency.

2. Construction of the heat engine or refrigerator

The heat engine or refrigerator is constructed of two d-dimensional thermo-chemical baths connected by two or more channels, as depicted in figure 1. The particles in the system have d degrees of freedom, equal positive charge e and equal mass m. We use units in which

J. Stat. Mech. (2011) P10026

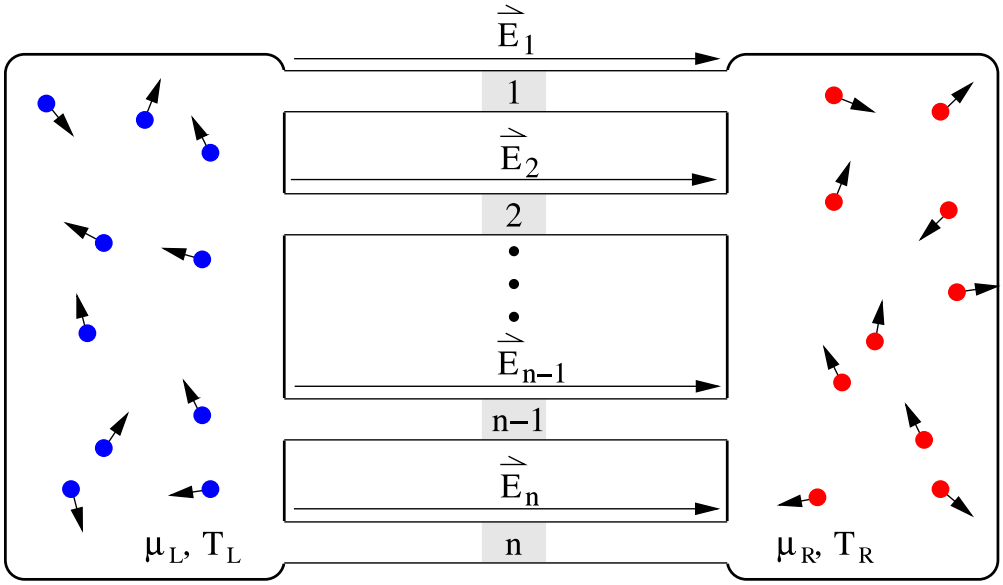

Figure 1. Schematic figure of the heat engine.

the charge e, mass m and Boltzmann constant k_B are equal to unity, $m = e = k_B = 1$. Along the direction of the channels we introduce bias electrical fields E_i, which are described by bias voltages U_i between the left and right baths. These voltages are used to extract work (or power) from the system in the case of a power-producing heat engine or to supply the work in the case of a refrigerator. The Hamiltonian H of a particle with momentum $p = (p_1, \ldots, p_d) \in \mathbb{R}^d$ and position $q = (q_1, \ldots, q_d) \in \mathbb{R}^d$ inside the ith channel is given by

$$H(q,p) = W(p) + U_i q_1, \qquad W(p) = \tfrac{1}{2}|p|^2.$$

The coordinate axis q_1 runs longitudinally along the channel, with units chosen so that $q_1 \in [0,1]$, where $q_1 = 0$ and 1 mark the left and right ends of the channel, respectively. Let there be n channels connecting the left bath side ($\nu = L$) with the right bath side ($\nu = \mathrm{R}$) via the holes $\Gamma_i \subset \mathbb{R}^{d-1}$ perpendicular (transverse) to the direction of the channel of 'area' $A_i = \Gamma_i$. For convenience we assume that the holes through which the channel i is attached to the left and right baths are represented by identical sets Γ_i (the analysis could easily be generalized if necessary). The total area of the holes is $A = \sum_{i=1}^{n} A_i$. The ratio $r_i = A_i/A$ represents the probability that a particle effused from the bath goes into the ith channel, from either side. The dynamics in each channel is reversible and energy conserving. The transmission function for a particle from side ν over the ith channel is defined as

$$\tau_{\nu,i}(x,p,U_i) = \begin{cases} 1: & \text{particle is effused at } x \in \Gamma_i \text{ with momentum } p \in \mathbb{R}^d \text{ from side } \nu \\ & \text{and transmitted through channel } i \text{ with bias voltage } U_i \\ 0: & \text{particle is reflected back into the same bath.} \end{cases} \tag{1}$$

A scheme for the explicit construction of the transmission functions is discussed in appendix A. In the left (right) bath the particles are at temperature T_L (T_R) and chemical

potential $\mu_{\rm L}$ ($\mu_{\rm R}$) and are effused into the ith channel at the rate $r_i\gamma_{\rm L}$ ($r_i\gamma_{\rm R}$). The effusion rates $\gamma_{\rm L}$ and $\gamma_{\rm R}$ are connected with the chemical potential μ_ν and reciprocal temperature β_ν via the formula

$$\beta\mu_\nu = \log\left(C\beta_\nu^{(d+1)/2}A_\nu\gamma_\nu\right), \qquad \nu \in {\rm L}, {\rm R},$$

where C is a constant depending only on the mass of the particles. The particles effused from ν-side bath at reciprocal temperature β into channels have momenta $p \in \mathbb{R}^d$ distributed according to the Boltzmann distribution

$$P(p,\sigma,\beta) = \beta\left(\frac{\beta}{2\pi}\right)^{(d-1)/2} |p_1| \exp\left(-\frac{1}{2}\beta|p|^2\right)\theta(\sigma p_1), \tag{2}$$

with unit step function $\theta(x) = (0 : x \leq 0; 1 : \text{otherwise})$. Let us now introduce the probability $t_{\nu,i}$ that a particle effused from side ν is transmitted over the ith channel, and the average particle kinetic energy $q_{\nu,i}$, which are computed as

$$(t_{\nu,i}, q_{\nu,i}) = \frac{1}{A_i}\int_{\mathbb{R}^d} {\rm d}p\, P(p,\sigma_\nu,\beta_\nu)(1, W(p)) \int_{\Gamma_i} {\rm d}x\, \tau_{\nu,i}(x,p,U_i), \tag{3}$$

with $\sigma_{\rm L} = 1$, $\sigma_{\rm R} = -1$. Notice that at equal temperatures $T_{\rm L} = T_{\rm R}$ and zero fields $U_i = 0$ we have $t_{{\rm L},i} = t_{{\rm R},i}$ and $q_{{\rm L},i} = q_{{\rm R},i}$. The particle currents $j_{\rho,i}$ within the ith channel and the heat currents $j_{q,i}|_\nu$ [3] exchanged between the ν-side bath and the ith channel are given by

$$j_{\rho,i} = r_i(\gamma_{\rm L}t_{{\rm L},i} - \gamma_{\rm R}t_{{\rm R},i}), \tag{4}$$

$$j_{q,i}|_{\rm L} = r_i\left(\gamma_{\rm L}q_{{\rm L},i} - \gamma_{\rm R}(q_{{\rm R},i} + t_{{\rm R},i}U_i)\right), \tag{5}$$

$$j_{q,i}|_{\rm R} = r_i\left(\gamma_{\rm L}(q_{{\rm L},i} - t_{{\rm L},i}U_i) - \gamma_{\rm R}q_{{\rm R},i}\right). \tag{6}$$

In the stationary state, the engine model should obey two basic principles (compatible, or even equivalence to the second law):

- The net particle current from one bath to another is zero $\sum_{i=1}^n j_{\rho,i} = 0$.
- If the temperatures of the baths are equal, then the particle current in each channel is zero.

Assuming that the average injection rate $\overline{\gamma} = \frac{1}{2}(\gamma_{\rm L} + \gamma_{\rm R})$ is known (say it is an input parameter of the model) the two above principles yield the relation

$$\frac{\gamma_{\rm R}}{\overline{\gamma}} - 1 = 1 - \frac{\gamma_{\rm L}}{\overline{\gamma}} = \frac{\mathcal{A}_{\rm L} - \mathcal{A}_{\rm R}}{\mathcal{A}_{\rm L} + \mathcal{A}_{\rm R}}$$

which up to a factor $\overline{\gamma}$ uniquely determines the injection rates $\gamma_{\rm L}$ and $\gamma_{\rm R}$. After introducing auxiliary variables

$$(\mathcal{A}_\nu, \mathcal{B}_\nu, \mathcal{C}_\nu) = \sum_{i=1}^n r_i(t_{\nu,i}, t_{\nu,i}U_i, q_{\nu,i}),$$

the stationary particle currents in the channels read

$$j_{\rho,i} = \frac{\overline{\gamma}r_i}{\mathcal{A}_{\rm L} + \mathcal{A}_{\rm R}}\left[t_{{\rm L},i}\mathcal{A}_{\rm R} - t_{{\rm R},i}\mathcal{A}_{\rm L}\right]$$

J. Stat. Mech. (2011) P10026

and the power produced by the particle flow is given by

$$P = \sum_{i=1}^{n} U_i j_{\rho,i} = \frac{\overline{\gamma} r_i}{\mathcal{A}_\mathrm{L} + \mathcal{A}_\mathrm{R}} \left[\mathcal{B}_\mathrm{L}\mathcal{A}_\mathrm{R} - \mathcal{B}_\mathrm{R}\mathcal{A}_\mathrm{L}\right].$$

A non-vanishing power is produced, if and only if $\mathcal{D} = \mathcal{B}_\mathrm{L}\mathcal{A}_\mathrm{R} - \mathcal{B}_\mathrm{R}\mathcal{A}_\mathrm{L}$ is non-zero. Similarly, we define the total stationary heat current $Q_\nu = \sum_{i=1}^{n} j_{q,i}|_\nu$ on both sides of the channels

$$Q_\mathrm{L} = \frac{2\overline{\gamma}}{\mathcal{A}_\mathrm{L} + \mathcal{A}_\mathrm{R}} \left[\mathcal{C}_\mathrm{L}\mathcal{A}_\mathrm{R} - \mathcal{C}_\mathrm{R}\mathcal{A}_\mathrm{L} + \mathcal{B}_\mathrm{R}\mathcal{A}_\mathrm{L}\right], \tag{7}$$

$$Q_\mathrm{R} = \frac{2\overline{\gamma}}{\mathcal{A}_\mathrm{L} + \mathcal{A}_\mathrm{R}} \left[\mathcal{C}_\mathrm{L}\mathcal{A}_\mathrm{R} - \mathcal{C}_\mathrm{R}\mathcal{A}_\mathrm{L} + \mathcal{B}_\mathrm{L}\mathcal{A}_\mathrm{R}\right]. \tag{8}$$

Notice the similar expression for the total heat current on the left and right side, which become identical in the linear temperature difference regime. We can think of the apparatus as a power-producing heat engine or as a refrigerator. In the heat engine regime, the heat is transferred from the hotter bath ν to the colder bath in such a way that the particles in the channels travel against the bias voltage and generate a power $P > 0$. In the case of the refrigerator regime, the heat is pumped from the colder bath of side ν, by appropriately setting the potentials in the channels, and thereby a power $P < 0$ is used. By introducing a binary index

$$\zeta = \begin{cases} +1: & \text{in the case of the power-producing heat engine mode} \\ -1: & \text{in the case of the refrigerator mode,} \end{cases}$$

we can write the efficiency η for both cases as

$$\eta = \left(\frac{\zeta P}{\sigma_\nu Q_\nu}\right)^{\zeta} \leq \eta_\mathrm{Carnot} = \left(\frac{|T_\mathrm{L} - T_\mathrm{R}|}{T_\nu}\right)^{\zeta}, \tag{9}$$

with $\sigma_\nu Q_\nu > 0$. The efficiency η of the heat engine and refrigerator is bounded from above by the efficiency of the ideal Carnot cycle η_Carnot. For a given setup of scatterers, the efficiency can be optimized by choosing appropriate potentials. In general, the optimization can be done only numerically, because the expressions for $t_{\nu,i}$ and $q_{\nu,i}$ are usually nonlinear functions of the potentials. Only in the linear temperature difference regime, discussed in section 3, can the optimization be done analytically.

3. Linear temperature difference regime

In section 2 we have discussed the general framework of our heat engine model. In the following we elaborate on the linear temperature difference regime, where the temperature difference $\delta T = T_\mathrm{R} - T_\mathrm{L}$ is much smaller than the average temperature $\overline{T} = \frac{1}{2}(T_\mathrm{L} + T_\mathrm{R})$. Consequently, the differences in the injection rates $\delta\gamma = \gamma_\mathrm{R} - \gamma_\mathrm{L}$ and electrical potentials U_i on both sides are also small. These conditions permit a perturbative treatment of energy and particle currents and enable an analytic optimization of the efficiency.

The idea is to expand the particle (4) and the heat currents (5) and (6), which depend on transport coefficients $t_{s,i}$ and $q_{s,i}$ (3) and injection rates γ_s, in terms of δT, $\delta\gamma$ and U_i. First we write the injection rates from both sides

$$\gamma_\nu = \overline{\gamma} + \tfrac{1}{2}\sigma_\nu \delta\gamma, \qquad \nu \in \{\mathrm{L}, \mathrm{R}\}$$

J. Stat. Mech. (2011) P10026

using the difference in injection rates $\delta\gamma$ reading

$$\delta\gamma = \overline{\gamma}\left[\left(\overline{\mu} - \frac{d+1}{2\overline{\beta}}\right)\delta\beta + \overline{\beta}\delta\mu\right] \tag{10}$$

where we introduce the average and the difference of the chemical potential $\overline{\mu} = (\mu_{\mathrm{L}} + \mu_{\mathrm{R}})/2$ and $\delta\mu = \mu_{\mathrm{R}} - \mu_{\mathrm{L}}$, respectively, and the reciprocal average temperature $\overline{\beta} = \overline{T}^{-1}$. Next we expand the transport coefficients $t_{s,i}$ and $q_{s,i}$ linearly in β and U_i around the equilibrium point $\beta = \overline{\beta}$, $U_i = 0$:

$$t_{\nu,i} = t_{\nu,i}|_0 + \partial_\beta t_{\nu,i}|_0\,\delta\beta + \sigma_\nu \partial_{U_i} t_{\nu,i}|_0\,U_i \tag{11}$$

$$q_{\nu,i} = q_{\nu,i}|_0 + \partial_\beta q_{\nu,i}|_0\,\delta\beta + \sigma_\nu \partial_{U_i} q_{\nu,i}|_0\,U_i. \tag{12}$$

Then, by using the transport coefficients computed at the equilibrium point—the average transmission probability $t_i^{(0)}$ and the first two moments of the kinetic energy transmitted per particle $q_i^{(0)}$ and $k_i^{(0)}$ given by

$$\left(t_i^{(0)}, q_i^{(0)}, k_i^{(0)}\right) = \frac{1}{A_i}\int_{\mathbb{R}^d} \mathrm{d}p\, P(p,1,\overline{\beta})(1, W(p), W(p)^2) \int_{\Gamma_i} \mathrm{d}x\, \tau_{\nu,i}(x,p,0), \tag{13}$$

we may write the temperature expansion coefficients as

$$\partial_\beta t_{\nu,i}|_0 = \frac{d+1}{2\overline{\beta}} t_i^{(0)} - q_i^{(0)}, \qquad \partial_\beta q_{\nu,i}|_0 = \frac{d+1}{2\overline{\beta}} q_i^{(0)} - k_i^{(0)}.$$

The latter depend only on the mean reciprocal temperature $\overline{\beta}$. For the time being we assume that the channels are straight cylindrical leads with a local scatterer in the middle (i.e. located in the center of each channel) and that the scattering process depends only on the kinetic energy, i.e.

$$\tau_{\nu,i}(x,p,U_i) := \psi_i\left(W(p) - \tfrac{1}{2}\sigma_\nu U_i\right)\theta\left(\tfrac{1}{2}p_1^2 - \max(0,\sigma_v U)\right), \tag{14}$$

where ψ is a transmission function at fixed energy of the scatterer inside the channel. We refer to ψ as the on-shell transmission function. It is possible to show that

$$\partial_{U_i} t_{\nu,i}|_0 = -\tfrac{1}{2}\sigma_\nu \overline{\beta} t_i^{(0)}, \qquad \partial_{U_i} q_{\nu,i}|_0 = -\tfrac{1}{2}\sigma_\nu(\overline{\beta} q_i^{(0)} - t_i^{(0)}) \tag{15}$$

and the transport coefficients at the equilibrium point simplify to

$$\left(t_i^{(0)}, q_i^{(0)}, k_i^{(0)}\right) = \frac{\overline{\beta}^{(d+1)/2}}{((d-1)/2)!}\int_0^\infty \mathrm{d}W\, W^{(d-1)/2}\,\mathrm{e}^{-\overline{\beta}W}\psi_i(W)(1, W, W^2). \tag{16}$$

The relations (15) are valid for scatterers of more general type even though it might be difficult to give a rigorous proof. In order to simplify the following discussion we introduce auxiliary constants

$$t_i = \overline{\gamma}\overline{\beta} r_i t_i^{(0)}, \qquad q_i = \overline{\gamma}\overline{\beta} r_i q_i^{(0)}, \qquad k_i = \overline{\gamma}\overline{\beta} r_i k_i^{(0)} \tag{17}$$

and the relative reciprocal temperature difference

$$\xi = \delta\beta/\overline{\beta}.$$

J. Stat. Mech. (2011) P10026

Taking into account the linear expansion of transport coefficients (15) and injection rates (10) we can write the particle currents $j_{\rho,i}$ (4) and the heat currents $j_{q,i}$ (5) as

$$j_{\rho,i} = -t_i(U_i + \delta\mu) + \xi q_i, \tag{18}$$

$$j_{q,i} = -q_i(U_i + \delta\mu) + \xi k_i, \tag{19}$$

where we use the fact that the heat currents on the left and right side are equal, $j_{q,i} := j_{q,i}|_{\mathrm{L}} = j_{q,i}|_{\mathrm{R}}$, in the considered regime. Without loss of generality, the mean value of the chemical potential $\overline{\mu}$ is set to zero, as only differences are important. The expression for the currents can be given in the matrix form

$$\begin{bmatrix} j_{\rho,i} \\ j_{q,i} \end{bmatrix} = \begin{bmatrix} t_i & q_i \\ q_i & k_i \end{bmatrix} \begin{bmatrix} -(U_i + \delta\mu) \\ \xi \end{bmatrix}, \tag{20}$$

showing that they indeed satisfy the Onsager reciprocity relations [3]. We express q_i and k_i in terms of positive quantities $S_i = q_i/t_i$ and $K_i = k_i - t_i S_i^2$. Note that t_i, K_i and S_i are proportional to the particle conductance, the heat conductance and the Seebeck coefficients of the ith channel, respectively. For further discussion it is convenient to introduce n-component column vectors

$$t = [t_i]_{i=1}^n, \qquad S = [S_i]_{i=1}^n, \qquad K = [K_i]_{i=1}^n, \qquad U = [U_i]_{i=1}^n, \qquad \underline{1} = [1, \ldots, 1]^T.$$

The stationary condition of zero net current $\sum_{i=1}^n j_{\rho,i} = 0$ determines the difference $\delta\mu$ of chemical potentials

$$\delta\mu = \frac{\xi t^T S - t^T U}{\underline{1}^T t}.$$

By using this result we write the stationary power $P = \sum_i j_{\rho,i}\delta U_i$ and the stationary net heat current $Q = \sum_i j_{q,i}$ as

$$P = (\xi S - U)^T M U, \qquad Q = \xi[S^T M S + (\underline{1}^T K)(\underline{1}^T t)] - MS$$

where the matrix $M = (\underline{1}^T t)\mathrm{diag}(t) - tt^T$. Notice that P and Q are invariant under the transformation $U \to U + \mathrm{const}$. The efficiency η (9) of the heat engine or refrigerator can be optimized w.r.t. to the field vector U by solving the set of equations $\partial\eta/\partial U = 0$. Let us introduce a quantity

$$y = \frac{S^T M S}{(\underline{1}^T K)(\underline{1}^T t)} > 0 \tag{21}$$

called the merit of efficiency of a heat engine. The dimensionless quantity y can be considered as an analog of the figure of merit ZT [3], used for characterizing material properties, which however here characterizes the entire engine composed possibly of many pieces. Then the optimal efficiency η^* of the heat engine or the refrigerator is equal to

$$\eta^* = \eta_{\mathrm{Carnot}} \frac{\sqrt{1+y} - 1}{\sqrt{1+y} + 1}, \tag{22}$$

J. Stat. Mech. (2011) P10026

and the corresponding vector of the bias voltages U^* and the output power P^* are written as

$$U^* = \xi \frac{\sqrt{1+y}}{y}\left(\sqrt{1+y}-\zeta\right)\left(S - \frac{1}{n}(\underline{1}^T S)\underline{1}\right), \tag{23}$$

$$P^* = -\left(\frac{\xi}{y}\right)^2 (S^T M S)\sqrt{1+y}\left(2\sqrt{1+y}-\zeta(2+y)\right), \tag{24}$$

$$Q^* = \zeta\frac{\xi}{y}(S^T M S)\sqrt{1+y}, \tag{25}$$

where we use for Carnot efficiency, $\eta_{\text{Carnot}} = \zeta\xi^\zeta$ (9). The relative efficiency $\eta/\eta_{\text{Carnot}}$ of the heat engine or refrigerator is a monotonically increasing function of y. In the limit $y \to \infty$, we reach the Carnot cycle efficiency. In the limit of two channels, $n = 2$, we obtain the expression already derived in [6, 7]. In this case the merit of efficiency reads

$$y = \frac{(S_1 - S_2)^2}{(K_1 + K_2)(1/t_1 + 1/t_2)}.$$

4. Optimally efficient engines

The efficiency of a steady state device that is working as a heat engine or refrigerator can be far from the maximal, Carnot cycle efficiency. Here we describe a general strategy to increase efficiency which is based on our model in the linear temperature difference regime.

Let us consider a n-channel heat engine or refrigerator with scattering depending only on the kinetic energy $\tau_{\nu,i}(x,p,0) = \psi_i(W(p))$, at reciprocal average temperature $\overline{\beta}$. We want to determine which properties of the scatterers may lead to maximal efficiency. By taking into account the transmission function and the distribution of momenta by the effusion process (2) we know that the particle's energy W transmitted over the ith channel has the probability density

$$P_i(W) = \frac{\overline{\beta}^{(d+1)/2}}{t_i^{(0)}\,((d+1)/2)!}\,\mathrm{e}^{-\overline{\beta}W} W^{(d-1)/2}\psi_i(W)$$

with average $\overline{W}_i = S_i$ and variance $V_i := \overline{W_i^2} - \overline{W_i}^2 = K_i/t_i$, where S_i, K_i and t_i are the transport coefficients introduced in section 3. It is interesting to note that in our notation the figure of merit ZT [5] of the ith channel is given simply by S_i^2/V_i.

In order to further simplify the discussion we assume that the bath openings are equal, $r_i =: r$, and that the scatterers have equal transmission probability, $t_i =: t$. This makes the channels comparable in their ability to transmit particles. In this case the merit of efficiency of our engine is simplified to

$$y = \frac{\sum_i S_i^2 - (1/n)(\sum_i S_i)^2}{\sum_i V_i}. \tag{26}$$

Imagine now that the scatterers act as energy window filters. Then, by narrowing the window, the variances V_i will decrease and the averages S_i will converge to some definite

J. Stat. Mech. (2011) P10026

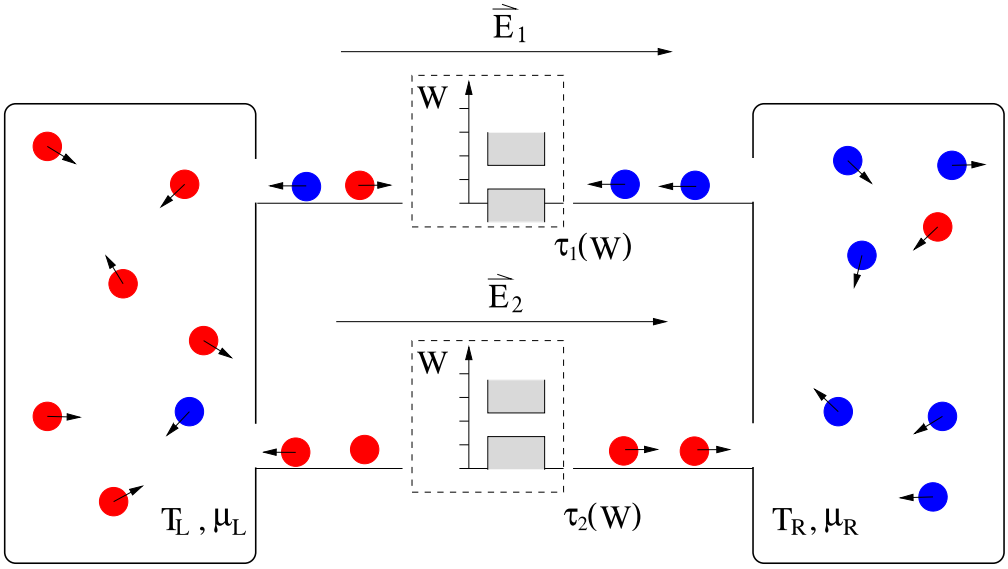

Figure 2. Schematic picture of the engine with the channel scatterers behaving as energy windows.

value. If the numerator in (26) does not vanish, then the merit of efficiency y will diverge and consequently

$$\lim_{V_i \to 0} \eta^* = \eta_{\text{Carnot}}. \tag{27}$$

We conclude that the efficiency of heat engines or refrigerators based on our model can be improved by strongly narrowing the energy window of transmission at the price of a smaller power output P^* or heat current Q^*, depending on the working regime. The idea of using narrow energy windows to improve thermoelectric efficiency is not new [2]. However, it is interesting that such a principle has a quite general validity.

5. Engine with a window-shape scatterers

Here we study a specific model of an engine (heat engine and refrigerator) with two ($n = 2$) one-dimensional ($d = 1$) channels with equal relative effusion probabilities, $r_1 = r_2 = \frac{1}{2}$. The particles are effused into channels from side ν with momentum $p \in \mathbb{R}$ distributed with probability density

$$P_\nu(p) = \beta |p| \mathrm{e}^{-(1/2)\beta p^2} \theta(\sigma_\nu p),$$

at reciprocal temperature β. In the middle of each channel there is a point-like scatterer, which allows transmission only of particles with kinetic energy in a specific interval and reflects all others. The on-shell transmission function of the scatterer ψ_i (14) in the ith channel has a window shape in the energy axis that is given by

$$\psi_i(W) = \theta(\chi_i + \Delta\chi_i - W)\theta(W - \chi_i),$$

where χ_i is the beginning of the energy window and $\Delta\chi_i$ is its width. This case is schematically depicted in figure 2.

The dynamics of the particles in the channels is conservative and symmetric w.r.t. time reversal. Due to the simplicity of the dynamics the transmission function of the channel (1) can be written explicitly and reads

$$\tau_{\nu,i}(x,p,U_i) = \psi_i(\tfrac{1}{2}p^2 - \tfrac{1}{2}\sigma_\nu U_i).$$

In the presence of an electric field, particles escape from the channels in a finite time, of order of magnitude $\mathrm{O}((\min_i |U_i|)^{-1/2})$. On the same time scale the engine relaxes into a non-equilibrium stationary state.

The performance of such engines can be evaluated analytically, but optimization, in general, can only be done numerically. In the following, we study engines in which the scatterers have transmission functions of the same width $\Delta\chi$. In particular, we set the electric field in the second channel to zero and optimize the efficiency by fine-tuning the electric field in the first channel. In figures 3 and 4 we show the optimal performances of the heat engine and the refrigerator, respectively, in the nonlinear temperature regime as a function of χ_i for two different $\Delta\chi$. In all cases, the optimal efficiency η^* and the optimal power P^* are zero on the diagonal $\chi_1 = \chi_2$, where scatterers in both channels are identical. Swapping of the parameters χ_1 and χ_2 corresponds to changing the currents' directions. In figure 3 we plot the optimal efficiency $\eta^*(\chi_1,\chi_2)$ and the corresponding power $P^*(\chi_1,\chi_2)$, which both turn out to be roughly symmetric functions. The symmetry is broken, as we apply the electric field just in the first channel. The optimal efficiency, near to Carnot's, is reached on an area lying parallel to the symmetry line $\chi_1 = \chi_2$ and, due to asymmetry in the setup, also along a steeper line $\chi_2/\chi_1 = \text{const}$. A high value of η^*, and with simultaneous high power output P^*, can be achieved in an area near to the χ_1 axis. Note that the maximal possible efficiency slightly increases on decreasing the widths $\Delta\chi$ of the energy windows in the scatterers. Apparently sharp, distinct regions of parameter space may suggest the existence of different regimes (phases) of transport, which might be characterized by different scalings with temperature. However, this is not investigated here.

The refrigerator is constructed similarly to the heat engine. The only difference is that we now apply an electric field to reverse the direction of the heat current so that the heat is sucked out by the engine at the cold bath $Q|_{\mathrm{L}} > 0$ (we take $T_{\mathrm{L}} < T_{\mathrm{R}}$), and thereby the bias voltage performs some work ($P < 0$). We find the optimal performance of the refrigerator by numerically maximizing the efficiency $\eta = Q|_{\mathrm{L}}/(-P)$ with the constraints $Q|_{\mathrm{L}} > 0$ and $P < 0$. This is not a trivial procedure and can easily fail if the optimal electric fields are either small or large. In figure 4 we present the relative optimal efficiency $\eta^*/\eta_{\mathrm{Carnot}}$ and the corresponding heat current Q^* as a function of the energy window thresholds χ_i in the nonlinear temperature regime. The results are shown for two widths $\Delta\chi$ of energy window. We see that the dependence of $\eta^*/\eta_{\mathrm{Carnot}}$ and P^* on parameters χ_i and $\Delta\chi$ is very similar to the case of the optimally performing heat engine, as expected from the linear theory. The area where the optimization fails, or where efficiency is negative, is shaded black and is located along the χ_2 axis. This show that the refrigerator cannot be realized for an arbitrary setup of scatterers.

In the linear temperature regime we are particularly interested in the limit of narrow energy windows. In this limit we can analytically compute the optimal efficiency η^* and the corresponding power P^* and heat current Q^* for arbitrary relative effusion probabilities r_i. Let us consider scatterers with energy windows of the same width

J. Stat. Mech. (2011) P10026

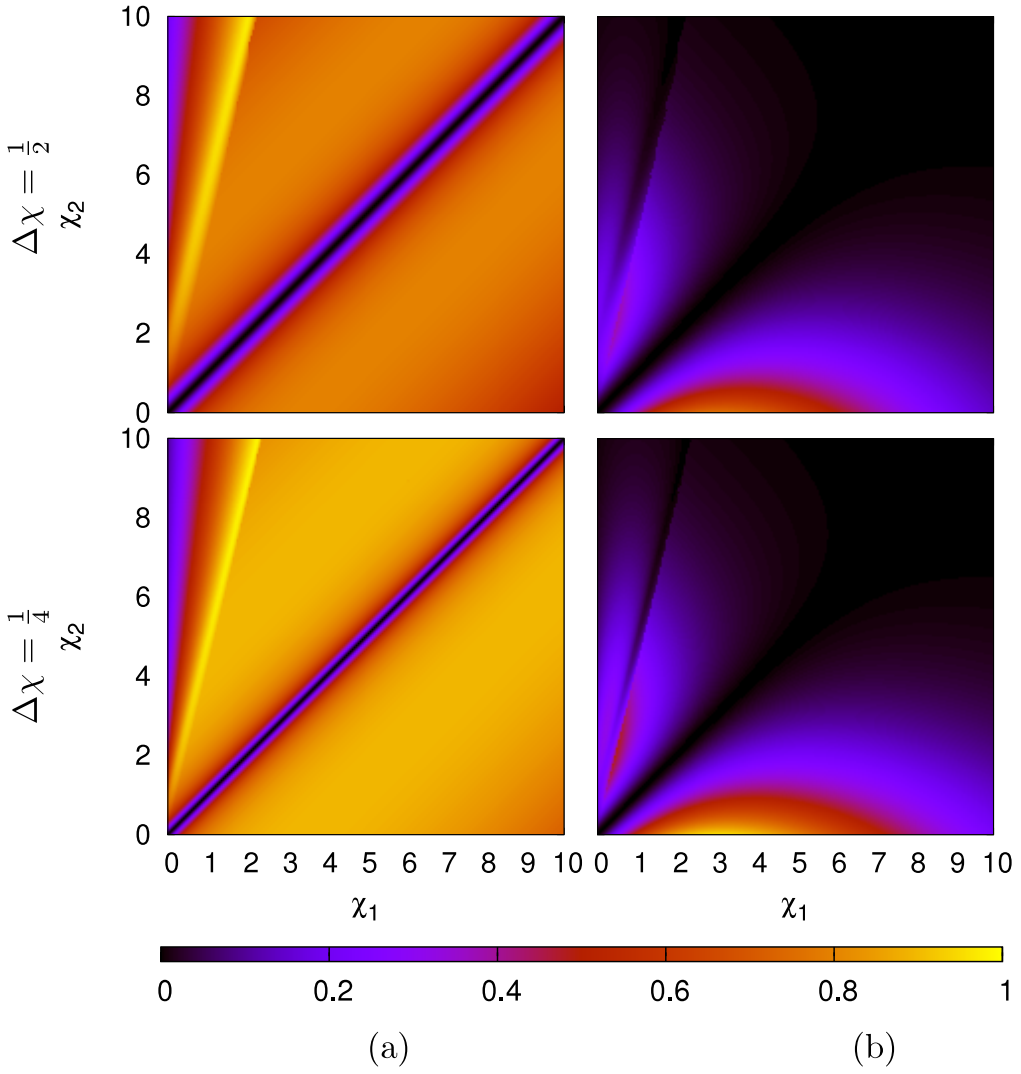

Figure 3. The relative optimal efficiency $\eta^*/\eta_{\mathrm{Carnot}}$ (a) and the corresponding rescaled power $a\,P^*/[\overline{T}(\eta_{\mathrm{Carnot}}\Delta\chi)^2]$ (b) of the heat engine at temperatures $T_{\mathrm{L}} = 1$ and $T_{\mathrm{R}} = 2$ ($\overline{T} = 3/2$) and $\overline{\gamma} = 1$ for two different widths of energy windows $\delta\chi$, where for convenience we take $a = 13$; here $\eta_{\mathrm{Carnot}} = \frac{1}{2}$.

$\Delta\chi$, and at mean energies $\overline{\chi}_1$ and $\overline{\chi}_2$ in the first and the second channel, respectively. In the discussed limit $\Delta x \to 0$ and for different fixed thresholds we may write

$$P^* = \frac{\overline{\gamma}\xi^2}{6\beta}[r_1\,\mathrm{e}^{-x_1} + r_2\,\mathrm{e}^{-x_2}]a(\Delta x)^2 + \mathrm{O}[(\Delta x)^3], \tag{28}$$

$$Q^* = \frac{\zeta\overline{\gamma}\xi}{6\beta}[r_1\,\mathrm{e}^{-x_1} + r_2\,\mathrm{e}^{-x_2}]a(\Delta x)^2 + \mathrm{O}[(\Delta x)^4], \tag{29}$$

$$\frac{\eta^*}{\eta_{\mathrm{Carnot}}} = 1 - \frac{\Delta x}{a} + \mathrm{O}[(\Delta x)^2], \tag{30}$$

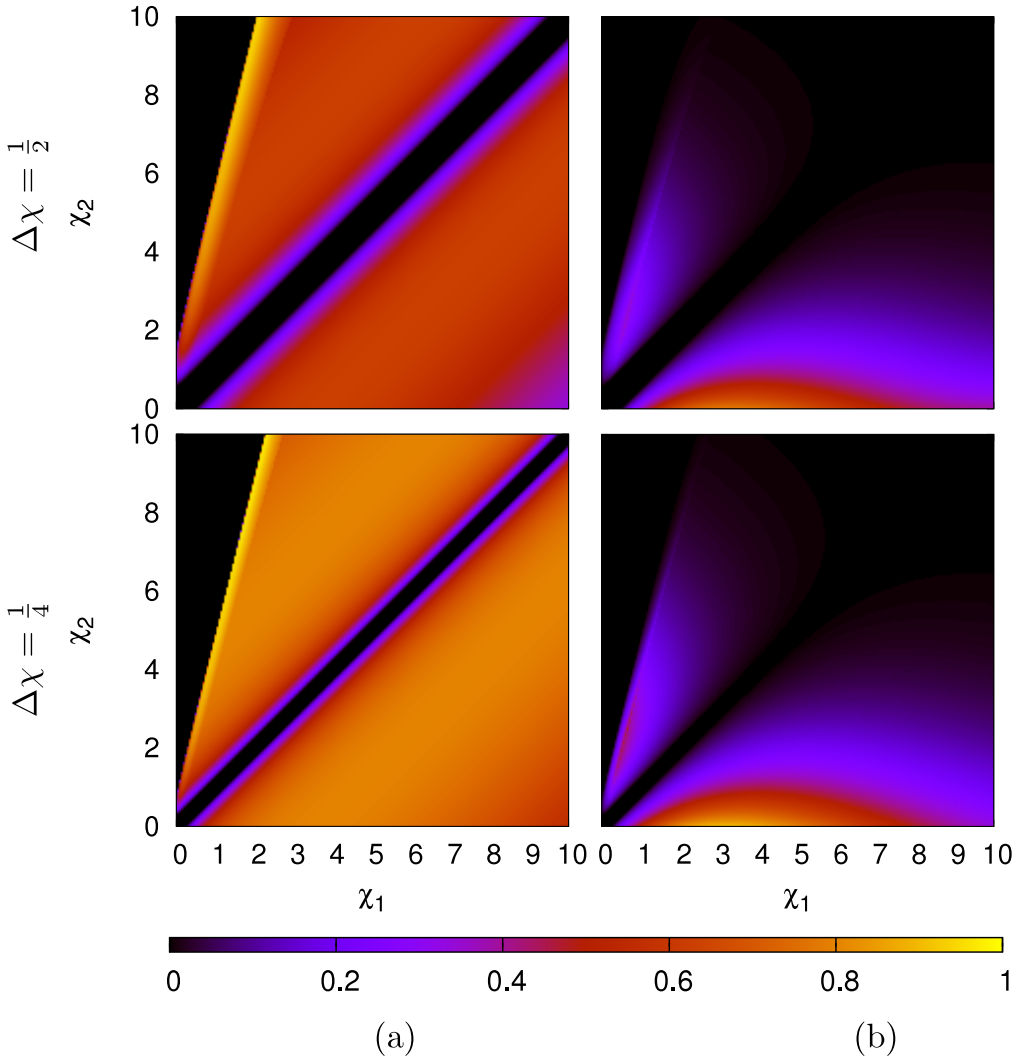

Figure 4. Refrigerator relative optimal efficiency $\eta^*/\eta_{\rm Carnot}$ (a) and corresponding heat current $45\,Q^*/(\overline{T}\eta^2_{\rm Carnot}\Delta\chi)$ (b). Here $\eta_{\rm Carnot} = 1$. For details see the caption under figure 3.

where we define rescaled window thresholds $x_i := \beta\chi_i$, rescaled widths $\Delta x := \beta\Delta\chi$, and a dimensionless scale

$$a = \frac{\sqrt{3}|x_2 - x_1|}{2\cosh\left[(1/2)\,(x_2 - x_1 + \log(r_1/r_2))\right]}.$$

The expressions (28)–(30) are valid only for $\Delta x < a$. It is clear that by decreasing the rescaled width Δx to zero, the efficiency η (30) increases linearly up to Carnot's value and the leading order of P^* (28) and Q^* (29) decrease quadratically to zero. Such behavior of the efficiency is expected and agrees with the result (27) and with the energy filtering mechanism discussed in the context of quantum mechanics [2, 4]. Note that the quantity a sets the typical size of the energy window width Δx, which is exponentially small when the threshold difference $|x_2 - x_1|$ is large, at which, i.e. when $\Delta x \lesssim a$, the efficiency becomes comparable to Carnot's.

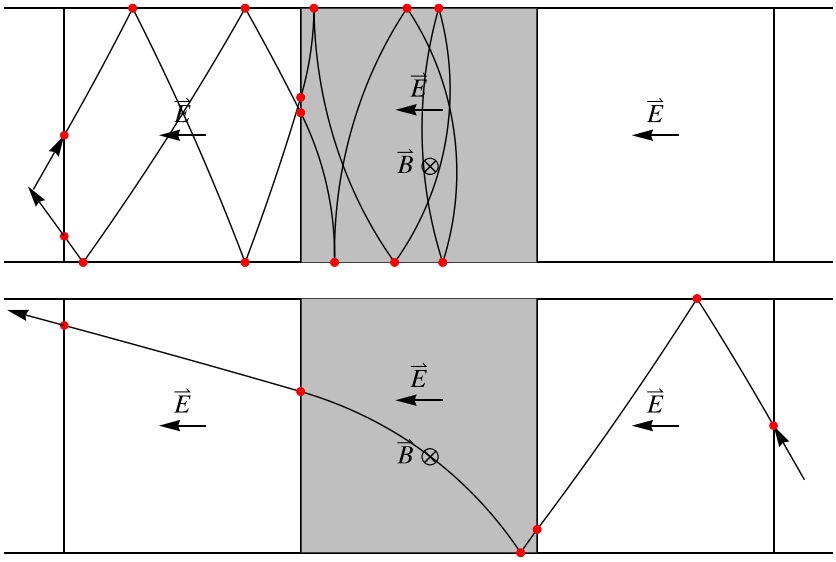

Figure 5. An illustration of trajectories in a channel with the middle section immersed into a transverse magnetic field. The lower panel shows the case of a trajectory effused from the other side.

6. Heat engine with magnetic fields

In this section, we consider a slightly different setup where time reversal invariance of the scattering mechanism is broken. We again take a model with two channels which are two dimensional $d = 2$ straight leads with hard walls. The ith channel is divided into three sections of lengths a_i, b_i and c_i (listed from left to right), see figure 5. The channel's length is $L = a_i + b_i + c_i$ and its width is h_i. The magnetic field B_i is applied to the middle section in the z direction and is described by the 'synchrotron orbital frequency'

$$\Omega_i = \frac{eB_i}{m},$$

where e and m are the charge and the mass of the particle, respectively. In addition to the magnetic field, we have a homogeneous electric field E_i along the channel, with voltage $U_i = -E_i L_i$ between the ends. The dynamics in the channels is energy conserving, but not symmetric w.r.t. time reversal. We may decompose the motion into bounces between channel boundaries of different sections that we may think of as nodes in a scattering graph. Then the scattering of particles is just a way to move in the scattering graph. In the considered case the scattering graph is infinite, due to the possibility of very small loops on the boundaries. However, the total length and time spent in these loops is proportional to the length of the boundaries and, therefore, is finite. Consequently, the particles in the presence of the electric field are ejected from the channels in a finite time.

The dynamics of particles in the lead has a certain symmetry. In the absence of an electric field each trajectory starting on the left side has a counterpart starting on the right side obtained by reflecting the trajectory through the center of the middle section. This means that at $E_i = 0$ and with equal bath temperatures $T_\mathrm{L} = T_\mathrm{R}$ we have $t_{\mathrm{L},i} = t_{\mathrm{R},i}$ and $q_{\mathrm{L},i} = q_{\mathrm{R},i}$. The transport coefficients $t_{\nu,i}$ and $q_{\nu,i}$ depend only on the absolute value

J. Stat. Mech. (2011) P10026

of the magnetic field. Indeed, a change in the sign of the magnetic field just mirrors the dynamics around the middle of the channel.

In the following we optimize the efficiency as a function of the electric field at the fixed orbital frequencies $\Omega_i > 0$. In numerical experiments the channels are taken of equal width, implying $r_1 = r_2 = \frac{1}{2}$, and with the unit average injection rate $\overline{\gamma} = 1$.

6.1. Linear temperature difference regime

In order to discuss the heat engine in the linear temperature difference regime using the linear expansion of currents (20) we have numerically checked the validity of equations (15). We calculate the transport coefficients $t_i^{(0)}$, $q_i^{(0)}$ and $k_i^{(0)}$ (13) at the mean reciprocal temperature $\overline{\beta} = 1/\overline{T}$ using the transmission function of the channels at zero electric field $\tau_{\nu,i}|_{U_i=0}$. The sections without the magnetic and electric field are perfect conductors and, therefore, transmission through the ith channel is determined by the transmission properties of the middle section, with the magnetic field of strength Ω_i, length b_i and width h_i. Consequently, the functions $\tau_{\nu,i}|_{U_i=0}$ in (13) can be replaced by the transmission function of the middle section $\tau_{\mathrm{B}}(y, p_x, p_y; \Omega_i, b_i, h_i)$ and we can write the transport coefficients as

$$(t_i^{(0)}, q_i^{(0)}, k_i^{(0)}) = \frac{1}{h_i}\int_0^{h_i} \mathrm{d}y \int_0^{\infty} \mathrm{d}p_x \int_{-\infty}^{\infty} \mathrm{d}p_x\, P(p;\overline{\beta})\tau_{\mathrm{B}}(y, p; \Omega_i, b_i, h_i)(1, W(p), W(p)^2)$$

where $p = (p_x, p_y)$ is the momentum and $W(p) = \frac{1}{2}(p_x^2 + p_y^2)$ is the kinetic energy of the particles effused into the channels. By closer analysis of the dynamics we find that transport coefficients can be conveniently expressed as

$$(t_i^{(0)}, q_i^{(0)}, k_i^{(0)}) = \frac{2\overline{\beta}^{3/2}}{\sqrt{\pi}} \int_0^{\infty} \mathrm{d}W\, W^{1/2}\, \mathrm{e}^{-\overline{\beta}W} \psi\left(\frac{W}{W_{0,i}}, \kappa_i\right)(1, W, W^2), \qquad (31)$$

with the on-shell transmission probability ψ defined as

$$\psi(w, \kappa) = \tfrac{1}{2}\int_0^1 \mathrm{d}y \int_{-1}^1 \mathrm{d}s\, \tau_{\mathrm{B}}\left(y, \sqrt{1-s^2}, s, \sqrt{w}, \kappa, 1\right),$$

where we introduce the energy scale $W_{0,i} = \frac{1}{2}(\Omega_i h_i)^2$ and the ratio between the length of the section and its width $\kappa_i = b_i/h_i$. The energy scale is proportional to the ratio between the critical temperature as defined in the paper [8] and the average bath temperature T. In general $\psi(w, \kappa)$ is a piecewise smooth function of both parameters, as we can see in figure 6. The shorter the section is in comparison to the width, the higher is the average transmission probability. As expected, the transmission probability at given w increases with decreasing κ. If the section with the magnetic field is longer than its width, then ψ becomes independent of κ, meaning

$$\psi(w, \kappa) = \psi(w, 1) \qquad \text{for } \kappa > 1.$$

Additionally, $\psi(w, \kappa)$ as a function w is independent of κ in the limit of small and large w. The asymptotic expansion in these two limits reads

$$\psi(w, \kappa) \sim \frac{\pi}{2} w^{1/2} \qquad w \to 0 \qquad \text{and} \qquad \psi(w, \kappa) \sim 1 - \frac{1}{24} w^{-1} + O(w^{-2}) \qquad w \to \infty.$$

J. Stat. Mech. (2011) P10026

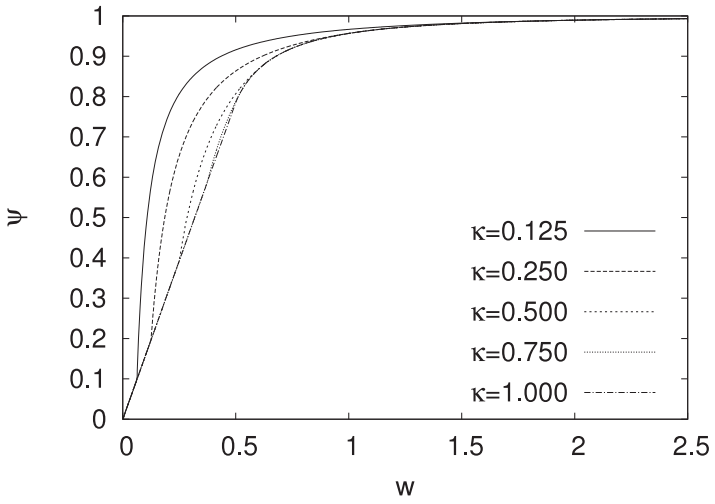

Figure 6. On-shell transmission $\psi(w, \kappa)$ through a channel with homogeneous magnetic field as a function of momentum $|p|$ for various κ.

In the absence of an electric field, ψ can be obtained analytically, but it is difficult. Nevertheless, we work here with a numerically computed ψ enhanced by analytical approximations. By using ψ to calculate coefficients (31), we study the optimal efficiency η^* and the corresponding power P^* of the heat engine given by equations (22) and (25), respectively, for different values of ratio κ. The results are shown in figure 7, where we plot η^* and P^* as a function of the rescaled energy scales $\kappa^2\overline{\beta}W_{0,i}$. Because the channels are identical, η^* and P^* are symmetrical on exchanging parameters. The areas of high optimal efficiency η^* and high power P^* overlap and are located along the abscissa and ordinate axes in $W_{0,1} \times W_{0,2}$ parameter space. For a given κ, the maximum of the optimal efficiency is achieved on the lines $(W_{0,1}, 0)$ and $(0, W_{0,2})$. The position of maximal optimal efficiency $W_{0,\max}$ and its value $\eta^*_{\max}$ depend on κ, as we see in figures 8(a) and (b). The maximal efficiency $\eta^*_{\max}$, and the relative energy scale $\overline{\beta}W_{0,\max}$ defining its position, increase as we decrease κ. Numerical calculations of $\eta^*_{\max}$ are difficult to perform for κ near to zero. In order to obtain results in this limit, we approximate the on-shell transmission probability with its approximate limiting form, given by

$$\psi(w,\kappa) \approx \psi_a(w,\kappa) = \begin{cases} \dfrac{\pi}{2} w^{1/2} : & w \leq \frac{1}{\pi^2}(1-\sqrt{1-\pi\kappa})^2 \\ 1 - \dfrac{1}{2}\kappa w^{-1/2} : & \text{otherwise,} \end{cases}$$

within a numerically determined absolute error $|\psi(w,\kappa) - \psi_a(w,\kappa)| < 5 \times 10^{-3}$ for $\kappa < 10^{-2}$. By using this approximation we see that the maximal optimal efficiency increases with decreasing κ, and converges in the limit $\kappa \to 0$ to its upper bound

$$\left.\frac{\eta^*_{\max}}{\eta_{\text{Carnot}}}\right|_{\kappa=0} = 0.0373 \pm 0.001,$$

at which the relative energy scale is $\kappa^2\overline{\beta}W_0 \sim 6.55 \pm 0.01$. Numerical results in figure 8(b) support this finding. We see that the maximal possible efficiency in the linear regime is below 4% of that achieved in the Carnot cycle.

J. Stat. Mech. (2011) P10026

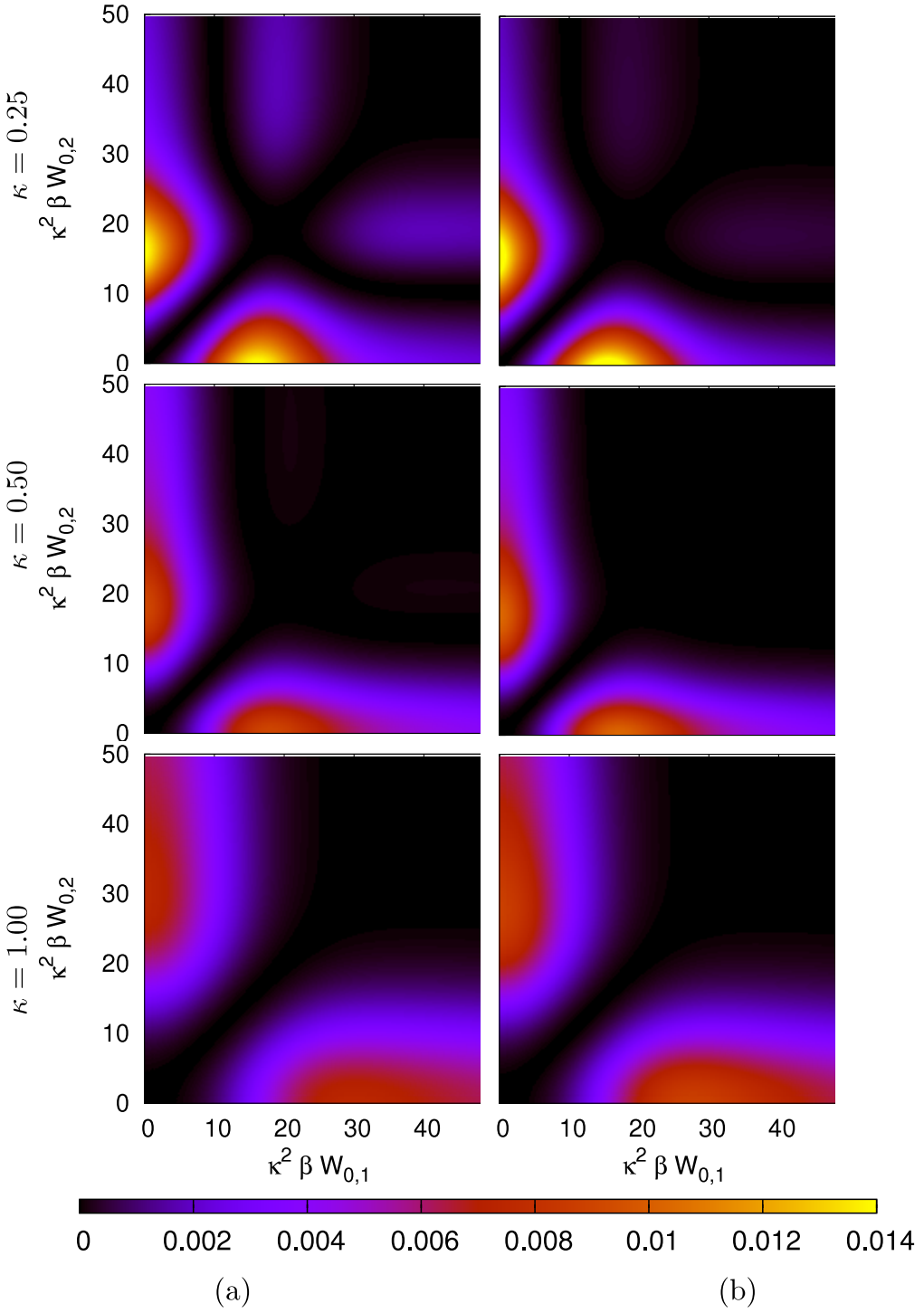

Figure 7. The relative optimal efficiency $\eta^*/\eta_{\mathrm{Carnot}}$ (a) and the corresponding rescaled power $P^*/(\eta^2_{\mathrm{Carnot}}\overline{T})$ (b) as a function of relative energy scales $\overline{\beta}\kappa^2 W_{0,i}$ at mean temperature $\overline{T} = 1$ for different values of κ.

J. Stat. Mech. (2011) P10026

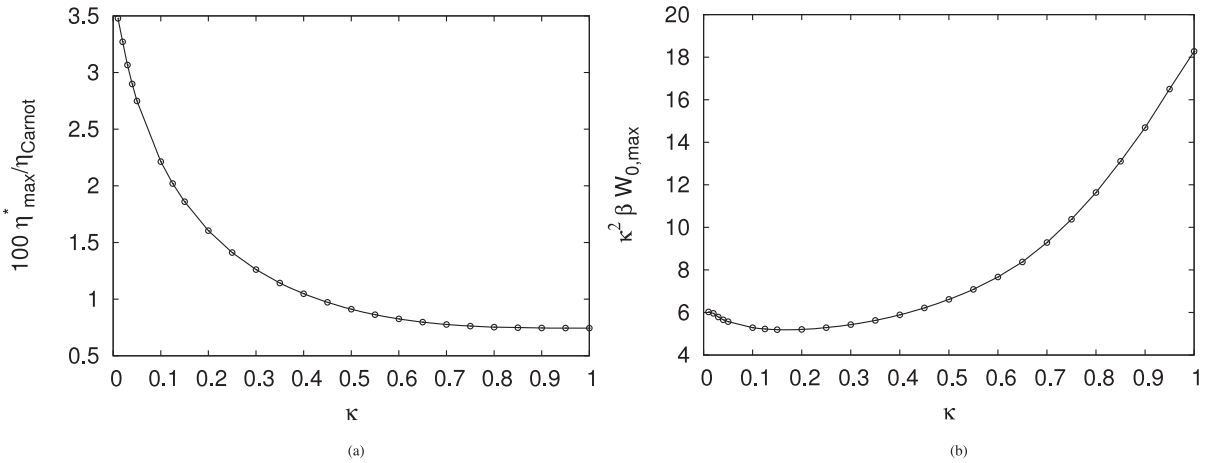

Figure 8. Relative maximal optimal efficiency $\eta^*_{\max}/\eta_{\text{Carnot}}$ (a) and its position βW_0 (b) for different values of κ.

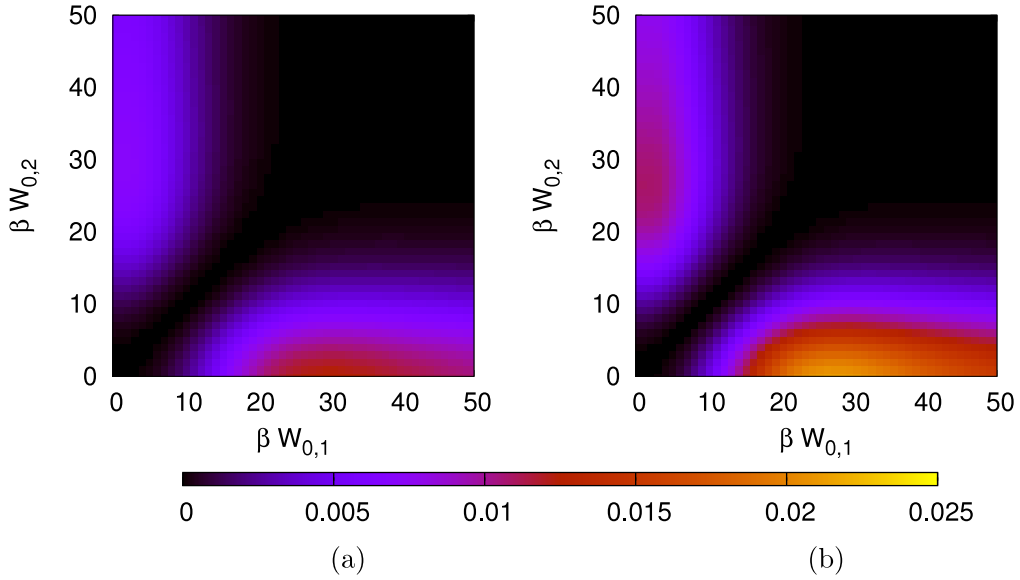

Figure 9. The relative optimal efficiency $\eta^*/\eta_{\text{Carnot}}$ (a) and the corresponding rescaled power $P^*/(\eta^2_{\text{Carnot}}\overline{T})$ (b) as a function of relative energy scales $\overline{\beta}W_{0,i}$ for temperatures $T_{\text{L}} = 0.55$ and $T_{\text{R}} = 1.45$, and their mean $\overline{T} = 1$.

6.2. Nonlinear temperature difference regime

In the nonlinear temperature regime, where $|T_{\text{L}} - T_{\text{R}}| \gtrsim \overline{T}$, we numerically obtain the transport coefficients $t_{\nu,i}$ and $q_{\nu,i}$ (3) and study the performance of the heat engine. In order to obtain the heat engine's optimal performance at fixed setup, we numerically find the optimal efficiency w.r.t. the electric potential U_i.

As an example, we present in figure 9 the optimal efficiency η^* and corresponding power P^* as functions of the relative energy scales $\beta W_{0,i}$ for $i = 1, 2$. In the example, the average temperature is $\overline{T} = 1$, the electric field is applied only in the first channel and the

J. Stat. Mech. (2011) P10026

lengths of the different sections and widths of the channel are equal, $a_i = b_i = c_i = h_i = 1$. In this setup we fix $\kappa_i = 1$. The η^* and P^* as functions of $\overline{\beta} W_{0,i}$ are slightly asymmetric, due to application of the bias voltage to the first channel only. Their functional dependence is not much different from that obtained in the linear temperature regime. We find that the relative maximal optimal efficiency $\eta^*_{\max}/\eta_{\rm Carnot}$ slightly increases when we increase the temperature difference between the baths. By increasing the temperature difference, at fixed average temperature, we also increase the power and heat current, since they are approximately proportional to $\eta_{\rm Carnot}$ and $\eta^2_{\rm Carnot}$, respectively.

7. Conclusions

We have demonstrated the operation of a thermoelectric heat engine and refrigerator in terms of a classical–mechanical model, which combines the deterministic classical scattering dynamics and stochastic heat reservoirs. The advantage of our simple model is that it is analytically treatable and allows for explicit exact results. In particular, we have been able to disclose various situations in which the efficiency can be close to Carnot's, and thus pose a promising alternative for technological application, in particular at the nanoscale, where the motion between the baths could be approximated by dissipationless dynamics.

Acknowledgments

We acknowledge financial support by the research grants Z1-0875 (MH) and J1-2208, P1-0044 (TP) of the Slovenian Research Agency (ARRS), and MIUR-PRIN 2008 and by Regione Lombardia. The authors thank the Max Planck Institute for the Physics of Complex Systems in Dresden for their hospitality in the Advanced Study Group 2010 during the finalization of the paper.

Appendix A. Calculating the classical scattering matrix

The channels joining the thermo-chemical baths are treated as two-port scatterers for particles of d degrees of freedom. Let us consider the ith channel connected to the left and right baths through openings in space $\Gamma_{{\rm L},i}$ and $\Gamma_{{\rm R},i}$, respectively, of an equal area $A_{{\rm L},i} = A_{{\rm R},i} =: A_i$. The transport properties of the channels are controlled via a homogeneous electric field with a voltage U_i between the ends. We imagine having a stationary transport in the channel, with particles being injected and ejected at both sides at constant rate. The probability density of positions and momenta of particles that are injected at side ν is given by

$$\rho_{{\rm in},\nu}(x,p) \qquad (x,p) \in \Gamma_{\nu,i} \times M_\nu,$$

where we introduce a momentum space for particles traveling in the ν direction $M_\nu = \mathbb{R}_{\sigma_\nu} \times \mathbb{R}^{d-1}$. Similarly, the probability density of particles ejected at side ν is

$$\rho_{{\rm out},\nu}(x,p) \qquad (x,p) \in \Gamma_{\nu,i} \times M_{\neg\nu}.$$

We assume $\rho_{{\rm in},\nu}(x,p) = 0$ for $\sigma_\nu p_1 < 0$ and $\rho_{{\rm out},\nu}(x,p) = 0$ for $\sigma_\nu p_1 > 0$. Using the introduced notation we may write that the probability density of ingoing particles $\rho_{\rm in}$ on

the phase space $V_{\mathrm{in},i} = (\Gamma_{\mathrm{L},i} \times M_{\mathrm{L}}) \cup (\Gamma_{\mathrm{R},i} \times M_{\mathrm{R}})$ and the probability density of outgoing particles ρ_{out} on the phase space $V_{\mathrm{out},i} = (\Gamma_{\mathrm{L},i} \times M_{\mathrm{R}}) \cup (\Gamma_{\mathrm{R},i} \times M_{\mathrm{L}})$ are defined as

$$\rho_{\mathrm{in}} = \rho_{\mathrm{in,L}} + \rho_{\mathrm{in,R}} \qquad \text{and} \qquad \rho_{\mathrm{out}} = \rho_{\mathrm{out,L}} + \rho_{\mathrm{out,R}},$$

respectively. The two-port classical scattering operator $\hat{S}$ associated with the channel is a linear map of ρ_{in} into ρ_{out}:

$$\rho_{\mathrm{out}} = \hat{S}\rho_{\mathrm{in}}.$$

The operator $\hat{S}$ depends on the dynamical properties of the channel. By using projectors $\hat{P}_\nu$, defined as $P_\nu f = \theta(\sigma_\nu p_1) f$, we can decompose the operator $\hat{S}$ into four operators:

$$\hat{T}_{\mathrm{L}} = \hat{P}_{\mathrm{L}}\hat{S}\hat{P}_{\mathrm{L}}, \qquad \hat{R}_{\mathrm{L}} = \hat{P}_{\mathrm{R}}\hat{S}\hat{P}_{\mathrm{L}}, \qquad \hat{T}_{\mathrm{R}} = \hat{P}_{\mathrm{R}}\hat{S}\hat{P}_{\mathrm{R}}, \qquad \hat{R}_{\mathrm{R}} = \hat{P}_{\mathrm{L}}\hat{S}\hat{P}_{\mathrm{R}}.$$

These operators describe (listed in the same order as above from left to right) the transmission from the left to the right side, the reflection from the left back to the left side, the transmission from the right to the left side and the reflection from the right back to the right side. Notice the sum of these operators is again the operator $\hat{S}$. The dynamics is deterministic and pointwise. Consequently, the trajectory's entry point $z = (x, p)$ can be uniquely connected to the exit point $z' = (x', p')$ via a map $z' = \phi(z)$, and $\hat{S}$ is a Koopman operator. This means $\hat{S}\delta'_z = \delta_{\phi(z')}$, where we use the Dirac delta $\delta'_z(z) := \delta(z - z')$. By using these facts we express the transmission function $\tau_{\nu,i}$ (1) as

$$\tau_{\nu,i}(x', p', U_i) = \int_{V_{\mathrm{out},i}} \mathrm{d}z\, (\hat{T}_\nu \delta_{z'})(z) = \int_{\Gamma_{\nu,i} \times M_{\neg\nu}} \mathrm{d}z\, (\hat{S}\delta_{z'})(z). \tag{A.1}$$

The transmission function $\tau_{\nu,i}$ of a channel is an essential ingredient of the presented theory of heat engines and refrigerators, and relation (A.1) connects it with a scattering operator $\hat{S}$. As we will show in the following, the operator $\hat{S}$ can be systematically obtained for structurally complicated channels, when scattering in its parts is known.

Let us assume that a channel can be divided into two parts with a common cross-section and simpler dynamics, which can be described by the scattering operators $\hat{S}_1$ and $\hat{S}_2$. The operator $\hat{S}_\nu$ can be decomposed into transmission and reflection operators $\hat{T}_{i,\nu}$ and $\hat{R}_{i,\nu}$. By knowing these, we can construct the transmission and reflection operators $\hat{T}_\nu$ and $\hat{R}_\nu$ corresponding to the scattering operator $\hat{S}$ of the whole channel via the concatenation formulas

$$\hat{R}_{\mathrm{L}} = \hat{R}_{1,\mathrm{L}} + \hat{T}_{1,\mathrm{R}}\hat{R}_{2,\mathrm{L}}\hat{L}^{-1}\hat{T}_{1,\mathrm{L}}, \qquad \hat{T}_{\mathrm{L}} = \hat{T}_{2,\mathrm{L}}\hat{L}^{-1}\hat{T}_{1,\mathrm{L}},$$

$$\hat{R}_{\mathrm{R}} = \hat{R}_{2,\mathrm{R}} + \hat{T}_{2,\mathrm{L}}\hat{R}_{1,\mathrm{R}}\hat{L'}^{-1}\hat{T}_{2,\mathrm{R}}, \qquad \hat{T}_{\mathrm{R}} = \hat{T}_{1,\mathrm{R}}\hat{L'}^{-1}\hat{T}_{2,\mathrm{R}},$$

with $\hat{L} = 1 - \hat{R}_{1,\mathrm{R}}\hat{R}_{2,\mathrm{L}}$ and $\hat{L}' = 1 - \hat{R}_{2,\mathrm{L}}\hat{R}_{1,\mathrm{R}}$. This is analogous to concatenation of quantum scattering matrices discussed in [9]. Note that the inverse operator $(1 - \hat{A})^{-1}$ is just an symbolic abbreviation for the series $\sum_{i=0}^{\infty} \hat{A}^i$. In order to simplify the writing we represent the concatenation of two scattering operators $\hat{S}_1$ and $\hat{S}_2$ into a resulting scattering operator S by a nonlinear and non-commutative product labeled by the symbol $\odot$, yielding

$$\hat{S} = \hat{S}_1 \odot \hat{S}_2.$$

doi:10.1088/1742-5468/2011/10/P10026

J. Stat. Mech. (2011) P10026

For example, let us consider a straight empty one-dimensional channel of length L, in the middle of which is a point scatterer that maps the incoming particle momentum p into $p' = O(\epsilon)p$, where O is an orthogonal matrix depending on the energy $\epsilon = \frac{1}{2}p^T p$. Such maps obey energy conservation. The scattering operator associated with empty wires of length $\frac{1}{2}L$, with voltage $\frac{1}{2}U$ between their ends, is defined as

$$(\hat{E}\phi)(p_1, p_2, \ldots, p_d) = \theta(-a)\phi(-p_1, p_2, \ldots, p_d) + \frac{|p_1|\theta(a)}{\sqrt{a}}\phi(\mathrm{sign}(p_1)\sqrt{a}, p_2, \ldots, p_d)$$

with $a = p_1^2 + \mathrm{sign}(p_1)U$. The scattering operator corresponding to the scatterer in the middle of the channel is written as

$$(\hat{P}\phi)(p) = \phi(O(\epsilon)^{-1}p).$$

Then we can write the scattering operator corresponding to the whole channel as a product

$$\hat{S} = \hat{E} \odot \hat{P} \odot \hat{E}.$$

The latter can be calculated systematically. Such kinds of channel are used for conduction of one-dimensional particles, where $O(\epsilon) \in \{-1, 1\}$, in a realization of the heat engine discussed in section 5.

Appendix B. Relaxation times

We consider a heat engine or refrigerator with multiple channels and no particles initially in the channels. Then, at time $t = 0$, the particles start to be injected into the channels from the left and right baths with the injection rates γ_L and γ_R, respectively. The number of particles in the channels $N(t)$ increases with time. Eventually it saturates to a stationary value such that the heat engine enters into a non-equilibrium stationary state. The characteristic time scales of this relaxation process are essential for practical implementations of heat engines and refrigerators. These can be obtained through the study of the functions $N(t)$, defined more precisely in the following.

Let us introduce the time function $\phi_{\nu,i}$, where $\phi_{\nu,i}(q,p) \geq 0$ represents the time needed for a particle entering the ith channel from side ν at the point $(q,p) \in \mathcal{V}_{\nu,i} = \Gamma_{\nu,i} \times M_\nu$ to return to the baths. The time function can be measured for the channels, and in some simple cases even analytically expressed. The number of particles in the ith channel coming form side ν is given by

$$N_{\nu,i}(t) = \frac{1}{A_{\nu,i}} \int_{\Gamma_{\nu,i}} \mathrm{d}q \int_{\mathbb{R}^d} \mathrm{d}p\, P(p, \sigma_\nu, \beta_\nu)\tau_{\nu,i}(q,p,U_i)\min(\phi_{\nu,i}(q,p), t). \quad \text{(B.1)}$$

Then the total number of particles in the channels is equal to

$$N(t) = \sum_{\nu,i} r_i \gamma_\nu N_{\nu,i}(t).$$

In order to obtain the relaxation time scales we need to understand the asymptotics of $N(t)$, which is determined by the effective injection rates $r_i\gamma_\nu$ and the asymptotics of the individual contributions $N_{\nu,i}$. It is difficult to say anything definite about the latter. But if $\phi_{\nu,i}$ is continuous except on $\mathcal{U}_{\nu,i} \subset \mathcal{V}_{\nu,i}$ of zero-measure then $N_{\nu,i}$ is also continuous. From definition (B.1) it is clear that $N(t)$ is non-constant in the limit $t \to \infty$, if $\phi_{\nu,i}$ has

J. Stat. Mech. (2011) P10026

a singularity on subset of $\mathcal{U}_{\nu,i}$. This nontrivial asymptotics of $N(t)$ is determined by the functional dependence of $\phi_{\nu,i}$ in the vicinity of $\mathcal{U}_{\nu,i}$.

As an illustration, let us consider an empty one-dimensional channel of length L with one-dimensional particles injected from one side at the rate γ. The time function ϕ of such a channel depends on the voltage U and reads

$$\phi(p) = \begin{cases} \dfrac{2L}{|p| + \sqrt{p^2 - u}} : & u < 0 \\ \theta(\sqrt{u} - |p|)\dfrac{2|p|L}{u} + \theta(|p| - \sqrt{u})\dfrac{2L}{p + \sqrt{p^2 + u}} : & \text{otherwise,} \end{cases}$$

with $u = 2\mathrm{sign}(p)U$. By using ϕ, we can compute the number of particles in the channel coming from one side $N_1(t)$ as a function of time t. In the presence of the electric field, ϕ is bounded from above by $t_0 = L/\sqrt{2|U|}$, which represents the time needed to achieve the stationary state. The stationary number of particles is $N_0 := \lim_{t\to\infty} N_1(t) \propto \gamma t_0$. In the absence of the field, $\phi(p)$ does not have an upper bound and behaves as $\phi(p) \asymp p^{-1}$ near $p = 0$. Consequently, the number of particles N_1 converges slowly in algebraic manner as

$$N_1(t) \asymp N_0 + \frac{t_1}{t}\left(\gamma t_1 - \frac{2N_0}{\sqrt{\pi}}\right) + O(t^{-3}),$$

with the stationary number $N_0 = \gamma L\sqrt{\beta\pi/2}$ and the time scale of relaxation $t_1 = L\sqrt{\beta/2}$. In view of these results, we expect that, in general, for channels composed of parallel walls in the absence of the field, the convergence towards the stationary state is algebraic. Therefore to achieve the stationary state in a finite time in such cases it is practical to apply electric fields in all channels.

References

[1] Mahan G D, Sales B and Sharp J, *Thermoelectric materials: new approaches to an old problem*, 1997 *Phys. Today* **50** 42

[2] Mahan G D and Sofo J D, *The best thermoelectric*, 1996 *Proc. Nat. Acad. Sci.* **93** 7436

[3] de Groot S R and Mazur P, 1962 *Nonequilibrium Thermodynamics* (Amsterdam: North-Holland)

[4] Humphrey T E and Linke H, *Reversible thermoelectric nanomaterials*, 2005 *Phys. Rev. Lett.* **94** 096601

[5] Casati G, Mejía-Monasterio C and Prosen T, *Increasing thermoelectric efficiency: a dynamical systems approach*, 2008 *Phys. Rev. Lett.* **101** 016601

[6] Horvat M, Prosen T and Casati G, *An exactly solvable model of a highly efficient thermoelectric engine*, 2009 *Phys. Rev.* E **80** 010102

[7] Wang J, Casati G, Prosen T and Lai C-H, *A one-dimensional hard-point gas as a thermoelectric engine*, 2009 *Phys. Rev.* E **80** 031136

[8] Casati G, Mejía-Monasterio C and Prosen T, *Magnetically induced thermal rectification*, 2007 *Phys. Rev. Lett.* **98** 104302

[9] Horvat M and Prosen T, *Dynamical approach to chains of scatterers*, 2007 *J. Phys. A: Math. Theor.* **40** 11593

[10] Saito K, Benenti G and Casati G, *A macroscopic mechanism for increasing thermoelectric efficiency*, 2010 *Chem. Phys.* **375** 508

J. Stat. Mech. (2011) P10026